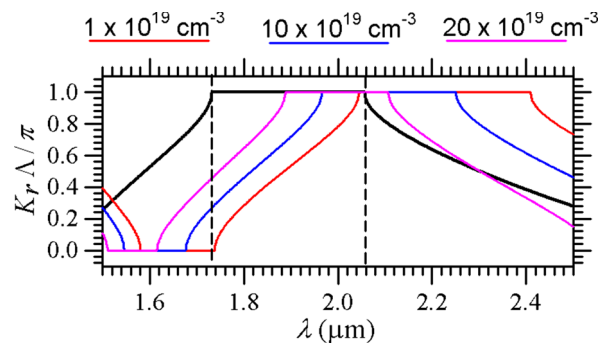


Tunable Multichannel Filter in a Photonic Crystal Containing Semiconductor Photonic Quantum Well

Volume 4, Number 1, February 2012

Hui-Chuan Hung
Chien-Jang Wu, Member, IEEE
Tzong-Jer Yang
Shoou-Jinn Chang, Senior Member, IEEE



DOI: 10.1109/JPHOT.2012.2186958
1943-0655/\$31.00 ©2012 IEEE

Tunable Multichannel Filter in a Photonic Crystal Containing Semiconductor Photonic Quantum Well

Hui-Chuan Hung,¹ Chien-Jang Wu,² *Member, IEEE*, Tzong-Jer Yang,³ and Shoou-Jinn Chang,¹ *Senior Member, IEEE*

¹Institute of Microelectronics and Department of Electrical Engineering, Center for Micro/Nano Science and Technology, Advanced Optoelectronic Technology Center, National Cheng Kung University, Tainan 701, Taiwan

²Institute of Electro-Optical Science and Technology, National Taiwan Normal University, Taipei 116, Taiwan

³Department of Electrical Engineering, Chung Hua University, Hsinchu 300, Taiwan

DOI: 10.1109/JPHOT.2012.2186958
1943-0655/\$31.00 ©2012 IEEE

Manuscript received December 1, 2011; accepted January 30, 2012. Date of publication February 3, 2012; date of current version February 17, 2012. This work was supported by the National Science Council (NSC) of Taiwan under Contract NSC-100-2112-M-003-005-MY3 and from the National Taiwan Normal University under NTNU100-D-01, as well as the NSC and Bureau of Energy, Ministry of Economic Affairs of Taiwan, under Contract NSC-100-2221-E-006-040-MY2 and 100-D0204-6 and the LED Lighting Research Center of National Cheng Kung University. Corresponding author: C.-J. Wu (e-mail: jasperwu@ntnu.edu.tw).

Abstract: A tunable multichannel filter in the finite photonic crystal (PC) containing photonic quantum well (PQW) as a defect is proposed. The symmetric structure $(AB)^P(CD)^Q(BA)^P$ and the asymmetric structure $(AB)^P(CD)^Q(AB)^P$ are considered in this work. Here, the host PC of $(AB)^P$ is made of Si for layer A and of SiO_2 for layer B. In the PQW, $(CD)^Q$, C also is Si, but D is an extrinsic semiconductor, n -type silicon (n -Si). With the use of n -Si, it is found that both structures can function as a tunable multichannel filter in the infrared region. The number of channels is equal to $Q + 1$ in the symmetric structure, whereas it is Q for the asymmetric one. The positions of multiple resonant peaks can be tuned by the variation in the impurity concentration of n -Si. The proposed filter could be used to design the wavelength division multiplexer filter that is of technical use in optical communications.

Index Terms: Photonic quantum well (PQW), multichannel filter, extrinsic semiconductor.

1. Introduction

Photonic crystals (PCs) are artificial media with periodic structures. Due to the periodic arrangement in structure, a PC possesses some photonic band gaps (PBGs) within which electromagnetic waves cannot propagate when their frequencies fall in the PBGs. These PBGs can be engineered for realizing some useful photonic devices. Among them, narrowband transmission filters (NTFs) are widely applied in photonics and optical communications. Using 1-D PC, an NTF is also called a multilayer Fabry–Perot resonator (FPR), which has a structure of $(AB)^P D (AB)^P$, where $(AB)^P$ is a finite PC, with A and B being the high- and low-index layer, respectively, D is the defect layer, and P is the stack number [1]. This NTF possesses a single transmission peak which, in general, can be designed in the vicinity of PBG center. With different material in D, filters with tunable feature can be obtained [2]–[6].

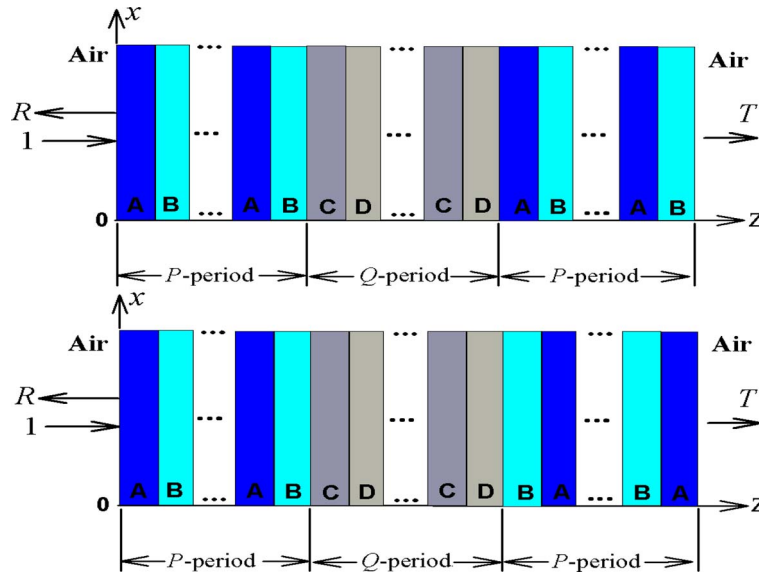


Fig. 1. Structures of a PC with a PQW-defect, in which the upper one $(AB)^P(CD)^Q(AB)^P$ is asymmetric and the lower one $(AB)^P(CD)^Q(BA)^P$ is said to be symmetric. The entire system is immersed in air. An optical wave with a unit power is normally incident at the left boundary, $z = 0$, and R and T are the reflectance and transmittance, respectively.

An NTF with multiple transmission peaks is more attractive in optical signal processing. For example, it can be designed a wavelength division multiplexer (WDM) filter that is of particular use in communications. To achieve a multichannel filter, the aforementioned structure has to be modified as $(AB)^P(CD)^Q(AB)^P$ or $(AB)^P(CD)^Q(BA)^P$, as depicted in Fig. 1. Here, the original defect layer, D, is replaced by the so-called photonic quantum well (PQW), $(CD)^Q$, with $Q < P$ [7]. In Fig. 1, the upper filter structure is said to be asymmetric whereas the lower one is referred to as a symmetric filter. In such a PQW PC structure, the design principle is that a pass band of PQW $(CD)^Q$ must be designed to be inside the PBG of host PC $(AB)^P$. Thus, when the structure, $(AB)^P(CD)^Q(AB)^P$, is formed, the continuous pass band will be quantized due to the photonic confinement. As a result, multiple discrete defect modes are created inside the PBG. Moreover, the number of defect modes (resonant peaks) is equal to Q [7]. The use of PQW as a defect layer in a PC provides a feasible method of designing PC multichannel filters [8]–[11].

In addition to the multiple-filtering feature, a tunable filter has attracted much attention in the community. The tuning can be made by means of external agents such as temperature (T-tuning), electric field (E-tuning), or magnetic field (M-tuning). For instance, using liquid crystal or superconducting material as a defect material, the filter belongs to T-tuning [12], [13]. As for the E-tuning filters, we mention references [2]–[6], [13]. With the use of magnetic material, an M-tuning tunable is obtained [14]–[16]. Another tunable filter called N-tuning can be achieved by using extrinsic semiconductor [17], [18]. In this case, the permittivity of extrinsic semiconductor is a function of the doping concentration, and consequently, the optical properties are tunable, tuned by the variation of the doping concentration.

The purpose of this paper is to design a tunable multichannel filter based on the use of PQW in a 1-D PC as well as the doped semiconductor. We shall consider two possible filter structures that are depicted in Fig. 1, in which a constituent of PQW, i.e., C, is taken to be the doped n -type extrinsic semiconductor n -Si. The tuning feature can be achieved by varying doping concentration in n -Si.

2. Basic Equations

For the PC with PQW in Fig. 1, all constituent layers are nonmagnetic, i.e., $\mu_A = \mu_B = \mu_C = \mu_D = 1$, and we take $A = \text{Si}$, $B = \text{SiO}_2$, $C = n\text{-Si}$, and $D = A = \text{Si}$. The relative permittivities of Si and

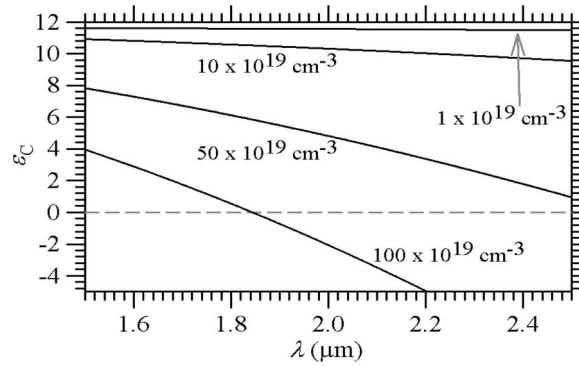


Fig. 2. Relative permittivity of *n*-Si versus wavelength at four distinct impurity concentrations.

SiO_2 are denoted as ε_A and ε_B , respectively. In the infrared region, the relative permittivity of *n*-Si can be described by the plasma model, namely [18]

$$\varepsilon_C(\omega) = \varepsilon_\infty \left(1 - \frac{\omega_{pe}^2}{\omega^2 - j\omega\gamma_e} - \frac{\omega_{ph}^2}{\omega^2 - j\omega\gamma_h} \right) \quad (1)$$

where $\varepsilon_\infty = 11.7$ is the high-frequency limit of the relative permittivity, γ_e and γ_h are the damping frequencies for the electrons and holes, respectively, and ω_{pe} , ω_{ph} are the electron and hole plasma frequencies given by

$$\omega_{pe,h} = \sqrt{\frac{n_{e,h}e^2}{m_{e,h}\varepsilon_0\varepsilon_\infty}} \quad (2)$$

Here, $m_{e,h}$ are respectively the effective masses of electron and hole. In addition, $n_{e,h}$ is the carrier concentration for *n*-type and *p*-type doped silicon, respectively. They can be determined from the law of conservation of charge, with the results [18]

$$n_e = \sqrt{n_i^2 + \frac{N^2}{4}} + \frac{N}{2} \quad n_h = \sqrt{n_i^2 + \frac{N^2}{4}} - \frac{N}{2} \quad (3)$$

where n_i is the intrinsic electron concentration of Si and N is the doping impurity concentration. It can be seen from (1)–(3) that the permittivity of *n*-Si is a function of frequency and doping concentration. Thus, the corresponding refractive index is given by

$$n_C(\omega, N) = \sqrt{\varepsilon_C(\omega, N)}. \quad (4)$$

In Fig. 2, we plot the wavelength-dependent permittivity of *n*-Si at near-infrared (1.5–2.5 μm) for four different impurity concentrations $N = 1 \times 10^{19}$, 10×10^{19} , 50×10^{19} , and $100 \times 10^{19} \text{ cm}^{-3}$. It can be seen that ε_C is a decreasing function of the wavelength. In addition, at a fixed wavelength, it decreases as impurity concentration increases. At higher concentration such as $100 \times 10^{18} \text{ cm}^{-3}$, the permittivity goes to a negative value, indicating that the strongly doped semiconductor behaves like a metal. With a negative permittivity, electromagnetic wave cannot propagate in a bulk material because it will be attenuated.

In what follows, properties of defect modes in two structures of Fig. 1, $\text{air}/(\text{AB})^P(\text{CD})^Q(\text{AB})^P/\text{air}$ (asymmetric), and $\text{air}/(\text{AB})^P(\text{CD})^Q(\text{BA})^P/\text{air}$ (symmetric), will be investigated. To analyze the defect modes, we shall calculate the wavelength-dependent transmittance, T , by making use of the transfer matrix method (TMM) [19]. First, we assume that time dependence is $\exp(j\omega t)$ for any field.

Then according to the TMM, the total transfer matrices for both systems $\text{air}/(AB)^P(CD)^Q(AB)^P/\text{air}$ and $\text{air}/(AB)^P(CD)^Q(BA)^P/\text{air}$ can be expressed as

$$M = \begin{pmatrix} M_{11} & M_{12} \\ M_{21} & M_{22} \end{pmatrix} = D_0^{-1} M_{AB}^P M_{CD}^Q M_{AB}^P D_0 \quad (5)$$

$$M = \begin{pmatrix} M_{11} & M_{12} \\ M_{21} & M_{22} \end{pmatrix} = D_0^{-1} M_{AB}^P M_{CD}^Q M_{BA}^P D_0 \quad (6)$$

respectively, where

$$M_{AB} = M_A M_B = D_A P_A D_A^{-1} D_B P_B D_B^{-1} \quad (7)$$

$$M_{BA} = M_B M_A = D_B P_B D_B^{-1} D_A P_A D_A^{-1} \quad (8)$$

$$M_{CD} = M_C M_D = D_C P_C D_C^{-1} D_D P_D D_D^{-1} \quad (9)$$

are the matrices of a single period in $(AB)^P$, $(AB)^P$, and $(CD)^Q$, respectively. Here, the dynamical matrix D_q ($q = 0, A, B, C, D$), is expressed as

$$D_q = \begin{pmatrix} 1 & 1 \\ n_q & -n_q \end{pmatrix} \quad (10)$$

where $q = 0$ is for air with $\varepsilon_0 = 1$. In (10), we have limited our study to the case of normal incidence as shown in Fig. 1. The propagation matrix P_i in (7)–(9) for layer i ($i = A, B, C, D$) takes the form

$$P_i = \begin{pmatrix} \exp(jk_i d_i) & 0 \\ 0 & \exp(-jk_i d_i) \end{pmatrix} \quad (11)$$

where d_i is the thickness of layer i and $k_i = n_i (2\pi/\lambda)$, is the associated wavenumber with n_i being the corresponding refractive index. The transmittance T can be calculated by the following equation:

$$T = \frac{1}{|M_{11}|^2}. \quad (12)$$

3. Numerical Results and Discussion

In order to achieve the function of multiple-filtering for the design structure of $(AB)^P(CD)^Q(AB)^P$, we have to first know the photonic band structures (PBSs) for both the infinite PCs of $(AB)^P$ and $(CD)^Q$ with $P \rightarrow \infty$ and $Q \rightarrow \infty$. The design rule is that a pass band of the PQW PC, $(CD)^Q$, must locate with a PBG of the host PC, $(AB)^P$. The PBS for a 1-D binary PC can be computed by the following central equation [19]:

$$\cos(K\Lambda) = \cos(k_1 d_1) \cos(k_2 d_2) - \frac{1}{2} \left(\frac{n_1}{n_2} + \frac{n_2}{n_1} \right) \sin(k_1 d_1) \sin(k_2 d_2) \quad (13)$$

where $\Lambda = d_1 + d_2$ is the spatial periodicity, and the Bloch wavenumber is defined as $K = K_r - jK_i$. For PQW (host) PC, we have $1 \rightarrow C(A)$ and $2 \rightarrow D(B)$. The pass band can exit where the solution is purely real, $K = K_r$. As for the PBG, solution for K must have an imaginary part K_i .

In Fig. 3, the PBSs of both PCs are plotted in the region of near-infrared (1.5–2.5 μm). Here, $\varepsilon_A = \varepsilon_D = 3.4$ (Si), $\varepsilon_B = 1.46$ (SiO_2), $d_A = 0.4$, $d_B = 1 \mu\text{m}$, are used for the PBS (black) of the host PC. As for the PQW PC, three PBSs are plotted, in which we choose $d_C = 0.8$ and $d_D = 0.42 \mu\text{m}$ for three different doping concentrations, $N = 1 \times 10^{19}$ (red), 10×10^{19} (blue), 20×10^{19} (purple) cm^{-3} . It can be seen that, at $N = 1 \times 10^{19} \text{cm}^{-3}$, a pass band of PQW PC is completely contained in the PBG of the host PC, which ranges from 1.736 to 2.058 μm . Thus, when PQW PC with $N = 1 \times 10^{19} \text{cm}^{-3}$ is sandwiched by two host PCs to form a filter structure, multiple transmission peaks inside the PBG can be expected to generate due to the photonic confinement. It what follows, we shall fixed the doping concentration at $N = 1 \times 10^{19} \text{cm}^{-3}$ for the filter structure of $(AB)^P(CD)^Q(AB)^P$.

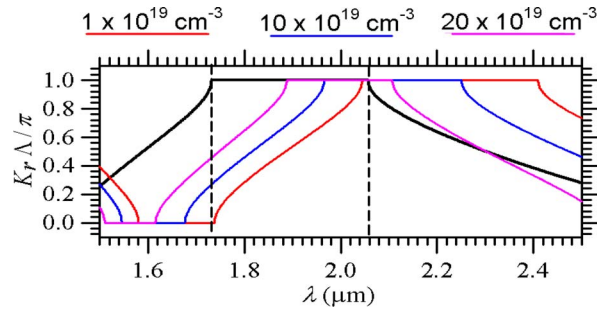


Fig. 3. Calculated PBSs for the ideal infinite host PC with a period of Si/SiO₂ (black curve) and PQC PC containing a period of *n*-Si/Si (red, blue, or purple curve). The region confined by two vertical dashed lines indicates a PBG of host PC, and a pass band (red) of PQC PC is contained in this PBG.

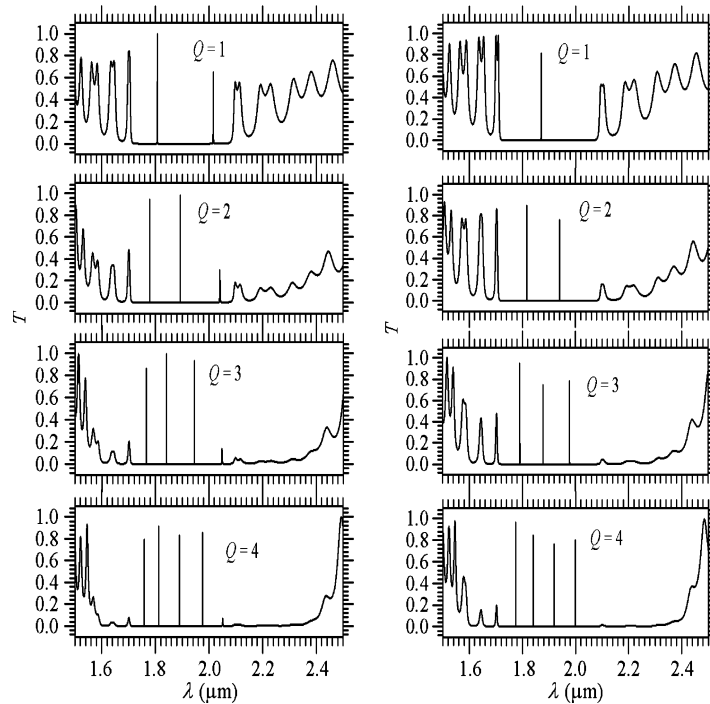


Fig. 4. Calculated wavelength-dependent transmittance for the filter structures, i.e., air/(AB)^P(CD)^Q(BA)^P/air (left), and air/(AB)^P(CD)^Q(AB)^P/air (right), at $Q = 1, 2, 3,$ and $4,$ respectively, and $P = 5.$ The multiple transmission peaks are produced due to the photonic confinement.

With the same material parameters in Fig. 3, in Fig. 4, we plot the calculated transmittance spectra for both the symmetric and asymmetric structures, i.e., air/(AB)^P(CD)^Q(BA)^P/air and air/(AB)^P(CD)^Q(AB)^P/air, at $P = 5$ for different stack numbers in PQC, $Q = 1, 2, 3,$ and $4.$ It can be seen that the number of multiple transmission peaks increases as Q increases. For a given $Q,$ there are $Q + 1$ transmission peaks in the symmetric structure. However, the number of peaks is Q for the asymmetric structure, which is consistent with the previous result [7]. The presence of multiple resonant peaks (or defect modes) is due to the photonic confinement. The PQC is sandwiched two mirrors and, thus, the continuous pass band in quantized into discrete peaks. In addition, these peaks do not have the same height that is different from that in [7]. This unequal resonant peak height can be ascribed to the wavelength-dependent permittivity in *n*-Si.

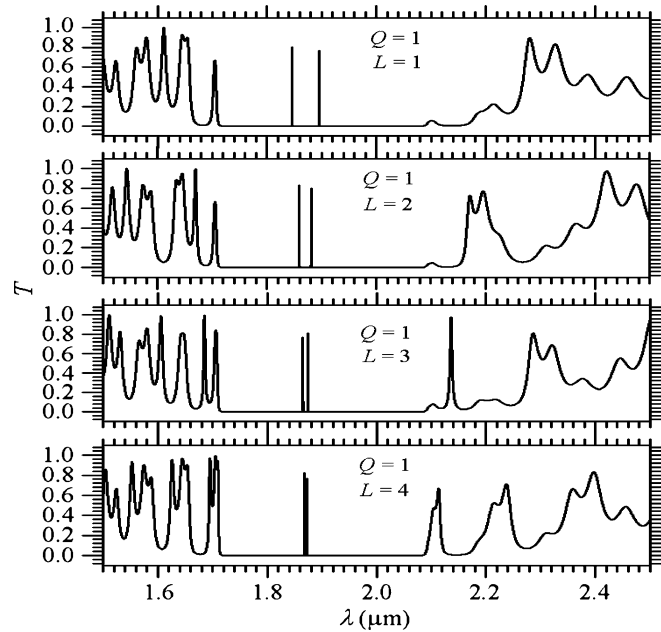


Fig. 5. Calculated wavelength-dependent transmittance for the filter structure containing DPQW, $\text{air}/(\text{AB})^P(\text{CD})^Q(\text{AB})^L(\text{CD})^Q(\text{AB})^P/\text{air}$ (right), at $L = 1, 2, 3$, and 4 , respectively, and $P = 5, Q = 1$. The single peak at $Q = 1$ in Fig. 4 is now split into two peaks due to the interaction between the two PQWs.

Let us now extend the above filter design by making use of the double photonic quantum wells (DPQWs). Based on the above asymmetric structure, the modified filter has a structure of $\text{air}/(\text{AB})^P(\text{CD})^Q(\text{AB})^L(\text{CD})^Q(\text{AB})^P/\text{air}$. Here, the middle $(\text{AB})^L$ plays as a coupling center between the DPQWs of $(\text{CD})^Q$ and its width is controlled by L . To compare with the result of single PQW in Fig. 4, $P = 5$ and $Q = 1$ are again taken here. In Fig. 5, we plot the transmittance spectra for this DPQW filter at different values, $L = 1, 2, 3$, and 4 . For an asymmetric filter containing a single PQW, there exists a single peak at $Q = 1$, as shown on the right side of Fig. 4. It can be seen from Fig. 5 that this single peak is split into two peaks when DPQW is used. Thus, the use of DPQW is advantageous to enhancing the filtering spectral efficiency since more resonant transmission peaks are generated inside the PBG. These two peaks can be ascribed to the interaction between DPQWs because of the existence of the coupling center $(\text{AB})^L$. It is also noted that the separation between two peaks is pronouncedly reduced as L increases. Increasing L weakens the interaction of two PQWs, and consequently, the two peaks are forced to be close together, as can be seen in the case of $L = 4$, in which the splitting becomes less apparent. In fact, these two peaks will merge together or become degenerate when $L = 5$. In this case, the entire structure can be regarded as two cascaded filters with the same peak position. The role played by the coupling center, which makes more peaks in the filter, is no longer valid. That is, the effect of coupling center can be evidently seen at $L < P$.

We continue to investigate how the peaks shift due to the variation of the doping concentration in layer C. For illustrative purpose, we consider the symmetric structure and take $Q = 1$ (and there are two peaks) as an example. In Fig. 6, the peak wavelengths at different impurity concentrations are given as follows:

N (cm^{-3})	Left peak (μm)	Right peak (μm)
1×10^{18}	1.811	2.018
1×10^{19}	1.807	2.016
2×10^{19}	1.803	2.013
3×10^{19}	1.799	2.011

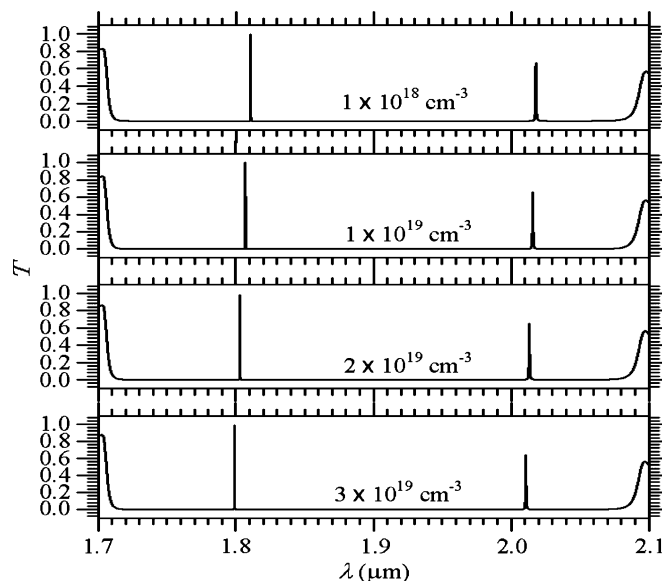


Fig. 6. Resonant peaks at $Q = 1$ in the symmetric structure for four different donor impurity concentrations of n -Si, $N = 1 \times 10^{18}$, 1×10^{19} , 2×10^{19} , and $3 \times 10^{19} \text{ cm}^{-3}$.

It can be seen that the positions of two peaks are slightly moved to the left, i.e., they have a tendency of blue-shift as the concentration increases.

Before giving a conclusion, it is worth mentioning the method of controlling doping concentration in fabrication. The uniformity of thickness and flatness of interfaces of both host PC and PQW in the path of electromagnetic wave are crucial. For thin layer epitaxy MOCVD shows the good performance to fabricate such a multiple-film PC. The procedures of fabrication are listed as follows: 1) to deposit an SiO_2 layer as stop layer on silicon substrate; 2) to deposit five Si/SiO_2 for the host PCs; 3) deposit $\text{Si}/n\text{-Si}$ PQW and five SiO_2/Si host PCs; 4) to deposit protection layer SiO_2 , which is the same thickness as the stop layer in Step 1; 5) to lithograph $200 \mu\text{m}$ square array at backside of silicon substrate; 6) to lithograph $200 \mu\text{m}$ square array on protection layer in Step 4; 7) to etch away silicon and stop on stop layer SiO_2 in Step 1; 8) to etch away SiO_2 on both sides; 9) to cut down the PC.

The crucial control during fabrication of multilayer is to maintain the deviation of each layer within acceptable variation: the flow rate of carrier gas, temperature of the reactor, and pressure needed to be in up/low limit. The clearness of substrate will strongly affect the uniformity and flatness of film. Most importantly, the impurity concentration in n -Si can be controlled by changing the flow rate of AsH_3 in Step 3.

4. Conclusion

In conclusion, a design of tunable and multiple channel filter operating in near-infrared region has been proposed. It is based on the use of PQW structure containing a doped semiconductor. The channel number is directly determined by the stack number in the PQW. With the increase in the impurity concentration, we find that these channels will be blue-shifted. The design structure can possess both multichannel as well as tuning features, which could be of technical use in the semiconductor photonic applications.

References

- [1] S. J. Orfanidis, *Electromagnetic Waves and Antennas*, Rutgers Univ., 2008. [Online]. Available: www.ece.rutgers.edu/~orfanidi/ewa
- [2] C.-J. Wu, J.-J. Liao, and T. W. Chang, "Tunable multilayer Fabry-Perot resonator using electro-optical defect layer," *J. Electromagn. Waves Appl.*, vol. 24, no. 4, pp. 531-542, 2010.

- [3] Q. Zhu and Y. Zhang, "Defect modes and wavelength tuning of one-dimensional photonic crystal with lithium niobate," *Optik*, vol. 120, no. 4, pp. 195–198, Feb. 2009.
- [4] X. Hu, Q. Gong, S. Feng, B. Cheng, and D. Zhang, "Tunable multichannel filter in nonlinear ferroelectric photonic crystal," *Opt. Commun.*, vol. 253, no. 1–3, pp. 138–144, Sep. 2005.
- [5] Y. K. Ha, Y. C. Yang, J. E. Kim, and H. Y. Park, "Tunable omnidirectional reflection bands and defect modes of a one-dimensional photonic band gap structure with liquid crystals," *Appl. Phys. Lett.*, vol. 79, no. 1, pp. 15–17, Jul. 2001.
- [6] Y. Q. Lu and J. J. Zheng, "Frequency tuning of optical parametric generator in periodically poled optical superlattice LiNbO₃ by electro-optic effect," *Appl. Phys. Lett.*, vol. 74, no. 1, pp. 123–125, Jan. 1999.
- [7] F. Qiao, C. Zhang, and J. Wan, "Photonic quantum-well structure: Multiple channeled filtering phenomena," *Appl. Phys. Lett.*, vol. 77, no. 23, pp. 3698–3700, Dec. 2000.
- [8] J. Liu, J. Sun, C. Huang, W. Hu, and D. Huang, "Optimizing the spectral efficiency of photonic quantum well structures," *Optik*, vol. 120, no. 1, pp. 35–39, Jan. 2009.
- [9] C. S. Feng, L. M. Mei, L. Z. Cai, P. Li, and X. L. Yang, "Resonant modes in quantum well structure of photonic crystals with different lattice constants," *Solid State Commun.*, vol. 135, no. 5, pp. 330–334, Aug. 2005.
- [10] J. Liu, J. Sun, C. Huang, W. Hu, and M. Chen, "Improvement of spectral efficiency based on spectral splitting in photonic quantum-well structures," *IET Optoelectron.*, vol. 2, no. 3, pp. 122–127, Jun. 2008.
- [11] Y.-H. Chang, C.-C. Liu, and C.-J. Wu, "Use of photonic quantum well as tunable defect in multilayer narrowband reflection-and-transmission filter," *Opt. Rev.*, vol. 17, no. 5, pp. 495–498, Sep. 2010.
- [12] I. L. Lyubchanskii, N. N. Dadoenkova, A. E. Zabolotin, Y. P. Lee, and Th. Rasing, "A one-dimensional photonic crystal with a superconducting defect layer," *J. Opt. A, Pure Appl. Opt.*, vol. 11, no. 11, p. 114 014, Sep. 2009.
- [13] P. Halevi, J. A. Reyes-Avendano, and J. A. Reyes-Cervantes, "Electrically tuned phase transition and band structure in a liquid-crystal-infilled photonic crystal," *Phys. Rev. E, Stat. Nonlinear Soft Matter Phys.*, vol. 73, no. 4, pt. 1, p. R040701, Apr. 2006.
- [14] H. Tian and J. Zi, "One-dimensional tunable photonic crystals by means of external magnetic fields," *Opt. Commun.*, vol. 252, no. 4–6, pp. 321–328, Aug. 2005.
- [15] M. Inoue, R. Fujikawa, A. Baryshev, A. Khanikaev, P. B. Lim, H. Uchida, O. Aktsipetrov, A. Fedyanin, T. Murzina, and A. Granovsky, "Magnetophotonic crystals," *J. Phys. D, Appl. Phys.*, vol. 39, no. 8, pp. R151–R161, Mar. 2006.
- [16] I. L. Lyubchanskii, N. N. Dadoenkova, M. I. Lyubchanskii, E. A. Shapovalov, and Th. Rasing, "Magnetic photonic crystals," *J. Phys. D, Appl. Phys.*, vol. 36, no. 18, pp. R277–R287, Sep. 2003.
- [17] E. Galindo-Linares, P. Halevi, and A. S. Sanchez, "Tuning of one-dimensional Si/SiO₂ photonic crystals at the wavelength of 1.54 μm ," *Solid State Commun.*, vol. 142, no. 1–2, pp. 67–70, Apr. 2007.
- [18] C.-J. Wu, Y.-C. Hsieh, and H.-T. Hsu, "Tunable photonic band gap in a doped semiconductor photonic crystal in near infrared region," *Prog. Electromagn. Res.*, vol. 114, pp. 271–283, 2011.
- [19] P. Yeh, *Optical Waves in Layered Media*. Singapore: Wiley, 1991.